Colossal Enhancement of Spin-Chirality-Related Hall Effect by Thermal Fluctuation

Yasuyuki Kato[*] and Hiroaki Ishizuka

Department of Applied Physics, The University of Tokyo, Bunkyo, Tokyo 113-8656, Japan

The effect of thermal fluctuation on the spin-chirality-induced anomalous Hall effect in itinerant magnets is studied theoretically. Considering a triangular-lattice model as an example, we find that a multiple-spin scattering induced by the fluctuating spins increases the Hall conductivity at a finite temperature. The temperature dependence of anomalous Hall conductivity is evaluated by a combination of an unbiased Monte Carlo simulation and perturbation theory. Our results show that the Hall conductivity can increase up to 10^3 times the ground-state value; we discuss that this is a consequence of a skew-scattering contribution. This enhancement shows that the thermal fluctuation significantly affects the spin-chirality-related Hall effect. Our results are potentially relevant to the thermal enhancement of the anomalous Hall effect often seen in experiments.

I. INTRODUCTION

The anomalous Hall effect (AHE) has been one of the central topics in the study of quantum-transport phenomena [1]. Continuous study over more than a century has revealed that the AHE shows rich properties, which attract interest not only with regard to basic science but also applications (e.g., high-accuracy Hall-effect sensors) [2,3]. Microscopically, the mechanism of the AHE is often classified into two groups: the intrinsic mechanism, related to the Berry curvature of the electronic bands [4], and the extrinsic mechanism, due to impurity scattering [5–7]. The difference in the microscopic origin is often reflected in the behavior of the AHE. For instance, the intrinsic AHE reflects singular structures in the Berry curvature. This gives rise to the nonmonotonic temperature (T) [8] and field [9] dependence of the anomalous Hall conductivity σ_{AHE}. On the other hand, the extrinsic AHE by magnetic scattering shows a peaklike enhancement of the Hall resistivity at a certain T that characterizes the underlying physics, such as the magnetic transition [10] and coherence [11–13] Ts. These rich features of the AHE have been intensively studied in both theory and experiment, and are also useful in identifying the physics behind the phenomena.

Among various studies, a recent breakthrough was the discovery of an AHE related to scalar spin chirality, which is often called the topological Hall effect (THE). The scalar spin chirality is a quantity defined by the scalar triple product of magnetic moments $\mathbf{S}_1 \cdot (\mathbf{S}_2 \times \mathbf{S}_3)$, where $\mathbf{S}_i$ is a local

magnetic moment [Fig. 1(a)]. This quantity is a measure of the noncoplanar nature of the spin texture, because the spin chirality is zero whenever the three spins lie in the same plane. It has been pointed out that the spins produce a fictitious magnetic field b when the three adjacent spins have a finite scalar spin chirality, resulting in an AHE [14–16] [Fig. 1(a)]. Alternatively, it is interpreted as an AHE due to the magnetic scattering by multiple scatterers [17,18]. The spin-chirality-related mechanism is studied in various materials, such as perovskite [19–22] and pyrochlore [16] oxides, chiral magnets [23–26], triangular oxides [27–31], and kagome antiferromagnets [32,33]. The THE in these materials is often investigated via the magnetic field dependence, which is consistent with the theoretical predictions [16,23,24].

In contrast, the T dependence of the THE in noncoplanar magnetic states is less understood. The Hall conductivity is expected to decrease with increasing temperature in magnets with noncoplanar magnetic orders because the scalar spin chirality decreases [curve B in Fig. 1(b)]. In experiments, however, many materials show an increase of the Hall conductivity with increasing T [25,30,31] [curve A of Fig. 1(b)]; some materials show the maximum slightly above the magnetic transition temperature T_c [30,31]. This is in contrast to the known theories, in which the maximum is expected to be below [10] or much [11] higher than T_c. No theoretical understanding on the T dependence has been reached so far.

In this work, we theoretically study the enhancement of Hall conductivity (σ_{THE}) by thermal fluctuation, focusing on fluctuation-induced skew scattering. As an example, we consider a triangular lattice model with a four-sublattice

————————
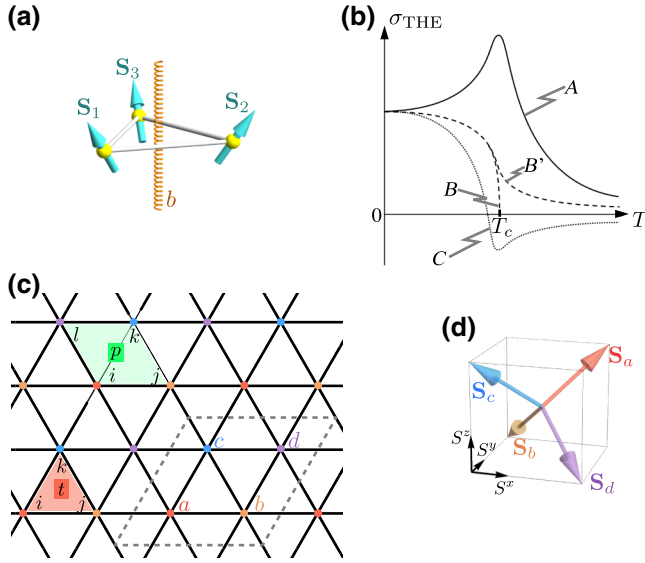*yasuyuki.kato@ap.t.u-tokyo.ac.jp

FIG. 1. The noncoplanar magnetic structure and the THE. (a) A schematic figure of the effective magnetic field induced by a noncoplanar magnetic structure. (b) A schematic figure for the T dependence of the anomalous Hall conductivity σ_{THE}. Curve B' (B) indicates the case in which σ_{THE} is proportional to the (spontaneous) scalar spin chirality, while curve C indicates the case with an extrinsic THE in chiral magnets [18]. In contrast, σ_{THE} in this study shows a different feature (curve A). (c) The triangular lattice model. The orange triangle (green plaquette) depicts the three-(four-)spins consisting of χ_p (h_p). The red, orange, blue, and purple sites indicate the a-, b-, c-, and d-sublattice structures of order $3Q$, respectively. (d) The spin orientation at each sublattice. All the spins in the ν-sublattice align with $\mathbf{S}_\nu$ at $T = 0$.

noncoplanar order called $3Q$ order [Figs. 1(c) and 1(d)]. The T dependence of σ_{THE} is calculated combining a Monte Carlo (MC) simulation and a large-size numerical calculation using the Kubo formula. We find that σ_{THE} increases with increasing T, sometimes up to 10^3 times compared with the ground state. The scan over the carrier density n_{el} ($0.1 \le n_{\text{el}} \le 1.9$), which is the average number of electrons per site, shows that the enhancement due to the skew scattering by multiple spins generally appears in this model. Our results show that the thermal fluctuation causes enhancement of the AHE at finite T.

II. MODEL

In this study, we consider a classical Heisenberg spin model on a triangular lattice as an example of short-range noncoplanar magnetic order [34]. The Hamiltonian reads as follows:

$$\mathcal{H}_{\text{spin}} = K \sum_p h_p + D_4 \sum_i [(S_i^x)^4 + (S_i^y)^4 + (S_i^z)^4]$$
$$- B_a \sum_{i \in a} \frac{S_i^x + S_i^y + S_i^z}{\sqrt{3}} - B_\chi \sum_t \chi_t, \quad (1)$$

where $\mathbf{S}_i$ ($|\mathbf{S}_i| = 1$) represents localized spin at site i, the sums $\sum_p$, $\sum_i$, and $\sum_t$ run over all the four-site plaquettes, all the sites, and all the three-site plaquettes, respectively, and K, D_4, B_a, and B_χ represent a short-range multispin interaction, a single-ion anisotropy, a sublattice specific magnetic field, and a fictitious field coupled to the spin chirality, respectively. For each triangular plaquette t and rhombic plaquette p, the multispin interactions are defined as follows:

$$h_{p=\{i,j,k,l\}} \equiv (\mathbf{S}_i \cdot \mathbf{S}_j)(\mathbf{S}_k \cdot \mathbf{S}_l) - (\mathbf{S}_i \cdot \mathbf{S}_l)(\mathbf{S}_j \cdot \mathbf{S}_k)$$
$$- (\mathbf{S}_i \cdot \mathbf{S}_k)(\mathbf{S}_j \cdot \mathbf{S}_l)$$
$$+ (\mathbf{S}_i \cdot \mathbf{S}_j + \mathbf{S}_i \cdot \mathbf{S}_k + \mathbf{S}_i \cdot \mathbf{S}_l + \mathbf{S}_j \cdot \mathbf{S}_k$$
$$+ \mathbf{S}_j \cdot \mathbf{S}_l + \mathbf{S}_k \cdot \mathbf{S}_l),$$
$$\chi_{t=\{i,j,k\}} \equiv \mathbf{S}_i \cdot (\mathbf{S}_j \times \mathbf{S}_k),$$

where $\{i, j, k\}$ of a triangular plaquette t is defined in counterclockwise order and $\{i, j, k, l\}$ of a rhombic plaquette p is defined so that the pairs of (i, k) and (j, l) are the diagonal pairs of the corners of a rhombic plaquette [see Fig. 1(c)]. A model with the first K term was originally introduced in a study on two-dimensional solid ^{3}He [35]. More recently, the biquadratic terms in h_p were discussed in the effective spin models for the Kondo lattice model [36,37]. The model with only K terms ($D_4 = B_a = B_\chi = 0$) exhibits a finite-T phase transition with the spontaneous Z_2 symmetry breaking from paramagnets to a chiral phase in which spins are disordered but χs are ordered [34].

With D_4, B_a, and B_χ, the low-T phase becomes a magnetic order because these terms reduce the symmetry: the D_4 term represents the single-spin cubic anisotropy, because of which the spins favor one of the $[\pm 1, \pm 1, \pm 1]$ directions ($D_4 > 0$); the B_a term represents the Zeeman coupling between the a-sublattice spins and an external magnetic field $\mathbf{B}_a \parallel [111]$ ($B_a > 0$), and the B_χ term represents a coupling between a fictitious field $B_\chi > 0$ and χ_t, because of which $\chi > 0$ over the entire T range. With these three terms, the low-T chiral phase is replaced by a four-sublattice long-range magnetic ordered phase [Figs. 1(c) and 1(d)]. In this state, the four spins on each sublattice in Fig. 1(c) point along different directions [Fig. 1(d)], forming a noncoplanar magnetic texture.

III. RESULTS

A. Monte Carlo simulation

The finite-T properties of this model are calculated by MC simulations using a standard single-spin-flip Metropolis algorithm [38]. Figure 2 shows the results of MC simulations with $\mathcal{H}_{\text{spin}}$. The specific heat C in Fig. 2(a) shows a peak at $T_c/K \simeq 2$ and the normalized structure factor $S(\pi, \pi)/N = \langle [(\sum_{i \in a,c} \mathbf{S}_i) - (\sum_{i \in b,d} \mathbf{S}_i)]^2 \rangle / N^2$ [where $N(= L^2)$ is the number of spins and L is the size of the
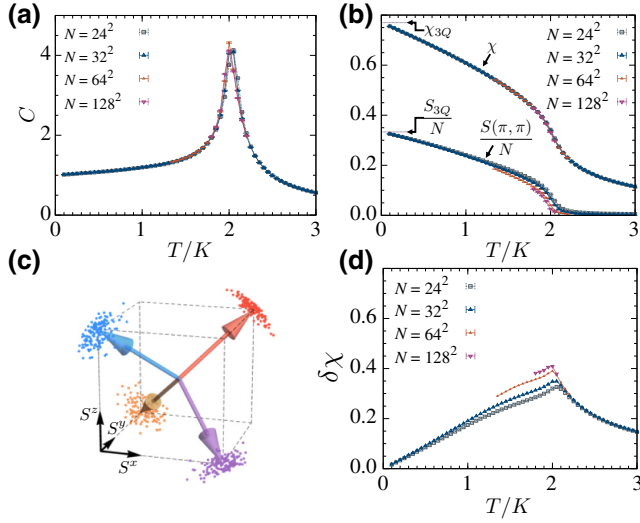
FIG. 2. The results of MC simulations of the model given in (1): (a) the specific heat C and (b) the normalized spin structure factor $S(\pi, \pi)/N$ and the scalar spin chirality χ. (c) A spin configuration in MC simulation at $T/K = 0.1$: each point represents a spin orientation and the arrows provide a visual guide. (d) The spin chirality of the fluctuating spins $\delta\chi$.

system] becomes nonzero below T_c, reflecting a phase transition to a magnetic order phase. At the lowest value of T, $S(\pi, \pi)/N$ approaches $S_{3Q}/N = 1/3$ and χ approaches $\chi_{3Q} = 4/(3\sqrt{3})$, as shown in Fig. 2(b). Figure 2(c) shows a spin configuration obtained in simulation at a sufficiently low value of T. These results consistently show that the ground state is the $3Q$ order and that the phase transition is continuous. We also find that the overall behavior of the above quantities converge sufficiently with $L \geq 24$, with some finite-size effect close to T_c. The behavior of C, $S(\pi, \pi)/N$, and χ, as well as the observed finite-size effect, indicate that the phase transition is continuous.

We note that the scalar spin chirality remains positive in the entire T range, even above T_c [Fig. 2(b)]. The nonzero χ comes from the local correlation of fluctuating spins under the B_χ field in Eq. (1), which acts as the "magnetic field" for χ. As a measure of the chirality due to the fluctuating spins, we use the following:

$$\delta\chi = \frac{\chi}{\chi_{3Q}} - \left[\frac{S(\pi, \pi)}{S_{3Q}}\right]^{3/2}. \qquad (2)$$

In contrast, $\delta\chi$ shows a different T dependence. Figure 2(d) shows that $\delta\chi$ increases with increasing T and shows a cusplike peak at T_c. The magnetic scattering due to fluctuating spins produces an AHE proportional to the scalar spin chirality [17,18]. Therefore, the fluctuating spins may produce a nonmonotonic T dependence of σ_{THE}.

B. Anomalous Hall conductivity

To study the T dependence of σ_{THE}, we consider itinerant electrons coupled to the spins in $\mathcal{H}_{spin}$. The electrons are coupled to the localized spins via Hund's coupling, i.e., we consider a Kondo lattice model on the triangular lattice. The Hamiltonian reads as follows:

$$\mathcal{H}_{KL} = -t \sum_{\langle i,j \rangle, s} (c_{is}^\dagger c_{js} + \text{h.c.}) - J \sum_{i,s,s'} \mathbf{S}_i \cdot (c_{is}^\dagger \boldsymbol{\sigma}_{ss'} c_{is'}), \qquad (3)$$

where $\boldsymbol{\sigma} = (\sigma^x, \sigma^y, \sigma^z)$ are the vector of Pauli matrices and $c_{is}^\dagger$ (c_{is}) is a creation (annihilation) operator of the itinerant electron at site i with spin s. The first term represents the kinetic energy term of the itinerant electrons and the second term the Hund's coupling. We assume that the coupling is relatively weak ($J = t/2$) and that the energy scale in the electron system is much larger than in the spin system. Then, for simplicity, we fix the temperature of the electron system $T_{el}/t = 0.025$. The Hall conductivity σ_{THE} is calculated by the Kubo formula using spin configurations generated by the MC simulation [38–43].

Figures 3(b) and 3(c) show $\sigma_{THE}(T)$ at $n_{el} = 0.3$ and 0.7 as examples. The different lines are for different choices of L and L_ϕ; we find only a small finite-size effect after taking the average over the twisted boundaries. When $n_{el} = 0.3$ [Fig. 3(b)], we find $\sigma_{THE} \sim 10^{-2} e^2/h$ at $T/T_c = 0.05 \ll 1$. However, σ_{THE} increases monotonically with increasing T, reaching $\sigma_{THE} \sim 0.3 e^2/h$ at $T \sim T_c$; this is approximately
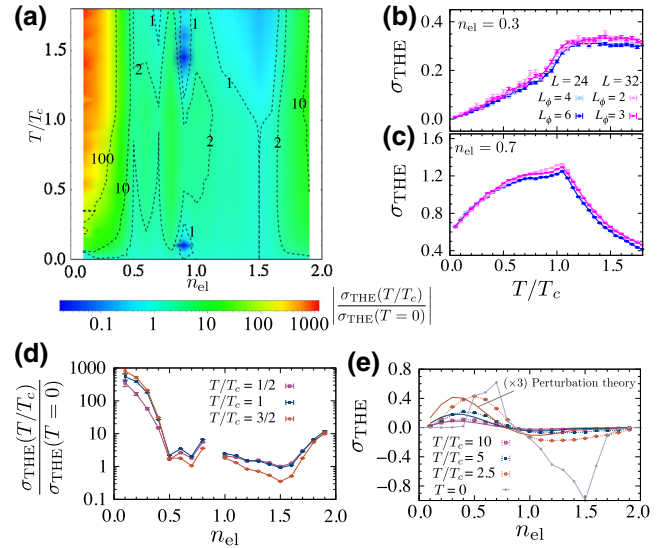

FIG. 3. The Hall conductivity σ_{THE} as a function of n_{el} and T. (a) A contour plot of $|\sigma_{THE}(T/T_c)/\sigma_{THE}(T = 0)|$ computed with $L = 32$ and $L_\phi = 3$. (b,c) $\sigma_{THE}(T/T_c)$ at $n_{el} = 0.3$ and 0.7. (d) The ratio of $\sigma_{THE}(T/T_c = 1/2, 1, \text{or } 3/2)$ and $\sigma_{THE}(T = 0)$ [44]. (e) The n_{el} dependence of $\sigma_{THE}(T \gg T_c)$ and $\sigma_{THE}(T = 0)$. The solid lines are obtained by perturbation theory, with a scale factor of 3 for visibility [17].

30 times larger than $\sigma_{\text{THE}}(T/T_c = 0.05)$. In our calculation, we find the enhancement of σ_{THE} in nearly all the choices of n_{el}. Figure 3(c) shows the results for $n_{\text{el}} = 0.7$. Similar to Fig. 3(b), σ_{THE} increases with increasing T and decreases above T_c; the curve shows a maximum around $T \sim T_c$ with a kink slightly below it. This trend also appears for $n_{\text{el}} > 1$, except for the difference in the sign of σ_{THE} [38].

The increase of σ_{THE} implies that the enhancement is related to the fluctuation effect. Indeed, the T dependence of σ_{THE} is in contrast to that of χ, which decreases monotonically with increasing T [Fig. 2(b)]. Therefore, the enhancement is different from what is expected in the intrinsic THE mechanism. On the other hand, the increase of σ_{THE} below T_c and the maximum around T_c are coincident with the T dependence of $\delta\chi$. Furthermore, at some filling, e.g., $n_{\text{el}} = 0.7$ [Fig. 3(c)], σ_{THE} shows a cusp at T_c resembling $\delta\chi$. These features imply that the enhancement is related to the spin chirality of the fluctuating spins $\delta\chi$, this presumably being related to the skew-scattering mechanism [18].

Our results in Fig. 3(a) also show that the thermal effect is larger when the Fermi level is close to the band edge, i.e., $n_{\text{el}} \sim 0$ or ~ 2. Figure 3(d) shows the ratio $\sigma_{\text{THE}}(T)/\sigma_{\text{THE}}(T = 0)$ at $T/T_c = 1/2$, 1, and 3/2. As shown in the figure, $\sigma_{\text{THE}}(T/T_c = 1/2, 1, 3/2)$ is typically 2–10 times larger than $\sigma_{\text{THE}}(T = 0)$. On the other hand, the enhancement at the band edges is much larger, sometimes up to 10^3 times that at $T = 0$.

The $n_{\text{el}} \sim 0$ and $n_{\text{el}} \sim 2$ regions are close to the ideal setup in which skew scattering is often studied. In the case $n_{\text{el}} \sim 0$ ($n_{\text{el}} \sim 2$), the electron (hole) bands are well approximated by the quadratic dispersion. The skew scattering in these situations is often driven by large-angle scattering, which is predominant when $\xi k_F \ll 1$. Here, k_F and ξ are the Fermi wave number and the correlation length for χ_t, respectively. Therefore, the skew-scattering theory in Ref. [18] applies to this case. The $\xi k_F \ll 1$ condition is not satisfied when the chemical potential moves away from the band edge. Hence, the results may generally change due to the large Fermi surface. Nevertheless, our result shows that the enhancement is commonly seen regardless of the size of the Fermi surface.

C. High-temperature region

We next turn to the n_{el} dependence of σ_{THE} at a high-T region well above T_c. The results of the MC simulation are shown in Fig. 3(e). They show a qualitatively different n_{el} dependence compared to the $T = 0$ result; σ_{THE} for $n_{\text{el}} < 1$ tends to be larger than that for $n_{\text{el}} > 1$ in the high T regime while the trend is opposite in the low T near $T = 0$. This contrasting trend at a high value of T is explained by the relaxation-time (the electron lifetime) dependence of the skew-scattering mechanism. To see the density-of-state

$[\rho(\mu)]$ dependence, we evaluate σ_{THE} using a perturbation method presented in Ref. [17]. In the $T \gg T_c$ region, the fluctuation contribution is expected to be the only contribution to the Hall effect. Also, the correlation length of the spins becomes very short in this region. Therefore, we only take into account the contribution from the nearest-neighbor spin correlation. With these approximations, the conductivity reads as follows [17]:

$$\sigma_{\text{THE}} = -\frac{e^2 J^3 \tau^2}{\pi N} \sum_{(ijk) \in t} \epsilon_{\alpha\beta\gamma} \langle S_{\mathbf{r}_k}^{\alpha} S_{\mathbf{r}_i}^{\beta} S_{\mathbf{r}_j}^{\gamma} \rangle$$
$$\times I_x(\mathbf{r}_j - \mathbf{r}_k) I_0(\mathbf{r}_k - \mathbf{r}_i) I_y(\mathbf{r}_i - \mathbf{r}_j), \qquad (4)$$

where $I_a(\mathbf{r}) \equiv (1/\tau N) \sum_{\mathbf{k}} v_{\mathbf{k}}^a e^{i\mathbf{k} \cdot \mathbf{r}}/(\varepsilon_{\mathbf{k}}^2 + 1/(4\tau^2))$ and $\mathbf{v_k}$ ($\varepsilon_{\mathbf{k}}$) is the velocity (energy) of electrons with momentum $\mathbf{k}$ ($v_{\mathbf{k}}^0 = 1$). Here, the sum of (ijk) is limited to the three spins forming the triangles t [Fig. 1(c)]. The electron lifetime τ is evaluated using the first Born approximation, $\tau^{-1}(\mu) = 2\pi J^2 \rho(\mu)$. Here, we neglect the spin-spin correlation for the evaluation of τ.

The result of Eq. (4) is shown in Fig. 3(e). The perturbation theory semiquantitatively reproduces the overall trend of the numerical results. The similarity between the numerical results and the perturbation suggests that the Hall effect is related to the skew scattering by the fluctuating spins in the high-T regime; in the perturbation theory, a larger skew-scattering contribution to σ_{THE} is expected when $\tau \propto \rho(\mu)$ is larger [2,17,18] and indeed $\rho(\mu)$ for $n_{\text{el}} < 1$ is smaller than that for $n_{\text{el}} > 1$.

IV. SUMMARY AND CONCLUDING REMARKS

To summarize, in this work, we study the effect of thermal fluctuation on the spin-chirality-related AHE. Through an unbiased numerical simulation, we find that the Hall conductivity σ_{THE} increases with increasing temperature, sometimes approximately 10^3 times the ground-state value. Detailed analysis of the temperature and electron-density dependence shows that the enhancement is consistent with the skew-scattering mechanism proposed recently [18]; the thermal enhancement is larger when the Fermi level is close to the band edge and is also related to the density of states. These results show a significant effect of the thermal fluctuation on the Hall effect induced by noncoplanar magnetic orders.

In contrast to our results, the skew-scattering mechanism is also discussed in relation to the sign change of σ_{THE} close to the critical temperature in chiral magnets with long-period magnetic orders (e.g., MnGe) [18]. This is a decidedly different behavior from the current case, in which the skew scattering enhances the Hall effect. Presumably, a key difference is the size of the magnetic structure, i.e., the characteristic wave number k^* is large (small) in order $3Q$ (magnetic skyrmion crystals). In the

skew-scattering mechanism [18], the scattering amplitude is proportional to $\sin\theta$, where θ is the angle between the incoming and outgoing electrons, i.e., larger-angle scattering is important. In addition to the skew scattering, small-angle scattering is also induced by the intrinsic THE when k^* is small. In other words, from the viewpoint of scattering theory, the scattering channels for the skew scattering and the intrinsic THE are different for small k^*. In contrast, since the magnetic unit cell of order $3Q$ has only four sites (k^* is large), both the skew scattering and the intrinsic THE induce large-angle scattering. Our results presented here show that magnetic fluctuations play a nontrivial and crucial role in magnets with such a short-period order.

ACKNOWLEDGMENTS

[1] Edwin Herbert Hall, XVIII. On the "rotational coefficient" in nickel and cobalt, Philos. Mag. **12**, 157 (1881).

[2] Naoto Nagaosa, Jairo Sinova, Shigeki Onoda, A. H. Mac-Donald, and N. P. Ong, Anomalous Hall effect, Rev. Mod. Phys. **82**, 1539 (2010).

[3] Sadamichi Maekawa, *Concepts in Spin Electronics* (Oxford University Press, Oxford, 2006).

[4] Robert Karplus and J. M. Luttinger, Hall effect in ferromagnetics, Phys. Rev. **95**, 1154 (1954).

[5] J. Smit, The spontaneous Hall effect in ferromagnetics I, Physica **21**, 877 (1955).

[6] J. Smit, The spontaneous Hall effect in ferromagnetics II, Physica **24**, 39 (1958).

[7] L. Berger, Side-jump mechanism for the Hall effect of ferromagnets, Phys. Rev. B **2**, 4559 (1970).

[8] Zhong Fang, Naoto Nagaosa, Kei S. Takahashi, Atsushi Asamitsu, Roland Mathieu, Takeshi Ogasawara, Hiroyuki Yamada, Masashi Kawasaki, Yoshinori Tokura, and Kiyoyuki Terakura, The anomalous Hall effect and magnetic monopoles in momentum space, Science **302**, 92 (2003).

[9] Kei S. Takahashi, Hiroaki Ishizuka, Tomoki Murata, Qing Y. Wang, Yoshinori Tokura, Naoto Nagaosa, and Masashi Kawasaki, Anomalous Hall effect derived from multiple Weyl nodes in high-mobility EuTiO$_3$ films, Sci. Adv. **4**, eaar7880 (2018).

[10] Jun Kondo, Anomalous Hall effect and magnetoresistance of ferromagnetic metals, Prog. Theor. Phys. **27**, 772 (1962).

[11] A. Fert and P. M. Levy, Theory of the Hall effect in heavy-fermion compounds, Phys. Rev. B **36**, 1907 (1987).

[12] Kosaku Yamada, Hiroshi Kontani, Hiroshi Kohno, and Satoru Inagaki, Anomalous Hall coefficient in heavy electron systems, Prog. Theor. Phys. **89**, 1155 (1993).

[13] Hiroshi Kontani and Kosaku Yamada, Theory of anomalous Hall effect in heavy fermion system, J. Phys. Soc. Jpn. **63**, 2627 (1994).

[14] Jinwu Ye, Y. B. Kim, A. J. Millis, B. I. Shraiman, P. Majumdar, and Z. Tešanović, Berry Phase Theory of the Anomalous Hall Effect: Application to Colossal Magnetoresistance Manganites, Phys. Rev. Lett. **83**, 3737 (1999).

[15] Kenya Ohgushi, Shuichi Murakami, and Naoto Nagaosa, Spin anisotropy and quantum Hall effect in the kagomé lattice: Chiral spin state based on a ferromagnet, Phys. Rev. B **62**, R6065 (2000).

[16] Y. Taguchi, Y. Oohara, H. Yoshizawa, N. Nagaosa, and Y. Tokura, Spin chirality, berry phase, and anomalous Hall effect in a frustrated ferromagnet, Science **291**, 2573 (2001).

[17] Gen Tatara and Hikaru Kawamura, Chirality-driven anomalous Hall effect in weak coupling regime, J. Phys. Soc. Jpn. **71**, 2613 (2002).

[18] Hiroaki Ishizuka and Naoto Nagaosa, Spin chirality induced skew scattering and anomalous Hall effect in chiral magnets, Sci. Adv. **4**, eaap9962 (2018).

[19] P. Matl, N. P. Ong, Y. F. Yan, Y. Q. Li, D. Studebaker, T. Baum, and G. Doubinina, Hall effect of the colossal magnetoresistance manganite La$_{1-x}$Ca$_x$MnO$_3$, Phys. Rev. B **57**, 10248 (1998).

[20] G. Jakob, F. Martin, W. Westerburg, and H. Adrian, Evidence of charge-carrier compensation effects in La$_{0.67}$Ca$_{0.33}$MnO$_3$, Phys. Rev. B **57**, 10252 (1998).

[21] S. H. Chun, M. B. Salamon, Y. Lyanda-Geller, P. M. Goldbart, and P. D. Han, Magnetotransport in Manganites and the Role of Quantal Phases: Theory and Experiment, Phys. Rev. Lett. **84**, 757 (2000).

[22] Y. Lyanda-Geller, S. H. Chun, M. B. Salamon, P. M. Goldbart, P. D. Han, Y. Tomioka, A. Asamitsu, and Y. Tokura, Charge transport in manganites: Hopping conduction, the anomalous Hall effect, and universal scaling, Phys. Rev. B **63**, 184426 (2001).

[23] A. Neubauer, C. Pfleiderer, B. Binz, A. Rosch, R. Ritz, P. G. Niklowitz, and P. Böni, Topological Hall Effect in the A Phase of MnSi, Phys. Rev. Lett. **102**, 186602 (2009).

[24] N. Kanazawa, Y. Onose, T. Arima, D. Okuyama, K. Ohoyama, S. Wakimoto, K. Kakurai, S. Ishiwata, and Y. Tokura, Large Topological Hall Effect in a Short-Period Helimagnet MnGe, Phys. Rev. Lett. **106**, 156603 (2011).

[25] T. Yokouchi, N. Kanazawa, A. Tsukazaki, Y. Kozuka, M. Kawasaki, M. Ichikawa, F. Kagawa, and Y. Tokura, Stability of two-dimensional skyrmions in thin films of Mn$_{1-x}$Fe$_x$Si investigated by the topological Hall effect, Phys. Rev. B **89**, 064416 (2014).

[26] C. Franz, F. Freimuth, A. Bauer, R. Ritz, C. Schnarr, C. Duvinage, T. Adams, S. Blügel, A. Rosch, Y. Mokrousov, and C. Pfleiderer, Real-Space and Reciprocal-Space Berry Phases in the Hall Effect of Mn$_{1-x}$Fe$_x$Si, Phys. Rev. Lett. **112**, 186601 (2014).

[27] Ivar Martin and C. D. Batista, Itinerant Electron-Driven Chiral Magnetic Ordering and Spontaneous Quantum Hall

Effect in Triangular Lattice Models, Phys. Rev. Lett. **101,** 156402 (2008).

[28] Yutaka Akagi and Yukitoshi Motome, Spin chirality ordering and anomalous Hall effect in the ferromagnetic Kondo lattice modelon a triangular lattice, J. Phys. Soc. Jpn. **79,** 083711 (2010).

[29] Yasuyuki Kato, Ivar Martin, and C. D. Batista, Stability of the Spontaneous Quantum Hall State in the Triangular Kondo-Lattice Model, Phys. Rev. Lett. **105,** 266405 (2010).

[30] Hiroshi Takatsu, Shingo Yonezawa, Satoshi Fujimoto, and Yoshiteru Maeno, Unconventional Anomalous Hall Effect in the Metallic Triangular-Lattice Magnet $PdCrO_2$, Phys. Rev. Lett. **105,** 137201 (2010).

[31] J. M. Ok, Y. J. Jo, Kyoo Kim, T. Shishidou, E. S. Choi, Han-Jin Noh, T. Oguchi, B. I. Min, and J. S. Kim, Quantum Oscillations of the Metallic Triangular-Lattice Antiferromagnet $PdCrO_2$, Phys. Rev. Lett. **111,** 176405 (2013).

[32] Hua Chen, Qian Niu, and A. H. MacDonald, Anomalous Hall Effect Arising from Noncollinear Antiferromagnetism, Phys. Rev. Lett. **112,** 017205 (2014).

[33] Satoru Nakatsuji, Naoki Kiyohara, and Tomoya Higo, Large anomalous Hall effect in a non-collinear antiferromagnet at room temperature, Nature **527,** 212 (2015).

[34] Tsutomu Momoi, Kenn Kubo, and Koji Niki, Possible Chiral Phase Transition in Two-Dimensional Solid ^{3}He, Phys. Rev. Lett. **79,** 2081 (1997).

[35] D. J. Thouless, Exchange in solid ^{3}He and the Heisenberg Hamiltonian, Proc. Phys. Soc. **86,** 893 (1965).

[36] Yutaka Akagi, Masafumi Udagawa, and Yukitoshi Motome, Hidden Multiple-Spin Interactions as an Origin of Spin Scalar Chiral Order in Frustrated Kondo Lattice Models, Phys. Rev. Lett. **108,** 096401 (2012).

[37] Hiroaki Ishizuka and Yukitoshi Motome, Strong coupling theory for electron-mediated interactions in double-exchange models, Phys. Rev. B **92,** 024415 (2015).

[38] See Supplemental Material http://link.aps.org/supple mental/10.1103/PhysRevApplied.12.021001 for the details of the Monte Carlo method, the Hall conductivity as a function of electron filling and temperature, the Monte Carlo simulations of spontaneous breaking of the scalar spin chirality, the calculations of Hall conductivity, and the perturbation theory. The supplemental material includes Refs. [45] and [46].

[39] Su Do Yi, Shigeki Onoda, Naoto Nagaosa, and Jung Hoon Han, Skyrmions and anomalous Hall effect in a Dzyaloshinskii-Moriya spiral magnet, Phys. Rev. B **80,** 054416 (2009).

[40] B. G. Ueland, C. F. Miclea, Yasuyuki Kato, O. Ayala-Valenzuela, R. D. McDonald, R. Okazaki, P. H. Tobash, M. A. Torrez, F. Ronning, R. Movshovich, Z. Fisk, E. D. Bauer, Ivar Martin, and J. D. Thompson, Controllable chirality-induced geometrical Hall effect in a frustrated highly correlated metal, Nat. Commun. **3,** 1067 (2012).

[41] Hiroaki Ishizuka and Yukitoshi Motome, Quantum anomalous Hall effect in kagome ice, Phys. Rev. B **87,** 081105(R) (2013).

[42] Hiroaki Ishizuka and Yukitoshi Motome, Spontaneous spatial inversion symmetry breaking and spin Hall effect in a spin-ice double-exchange model, Phys. Rev. B **88,** 100402(R) (2013).

[43] H. D. Rosales, F. A. Gómez Albarracń, and P. Pujol, From frustrated magnetism to spontaneous Chern insulators, Phys. Rev. B **99,** 035163 (2019).

[44] The results for $n_{el} = 0.9$ are not shown because of large numerical errors.

[45] Yukitoshi Motome and Nobuo Furukawa, Ferromagnetic transition in the double-exchange model on the pyrochlore lattice, J. Phys.: Conf. Ser. **200,** 012131 (2010).

[46] Kipton Barros and Yasuyuki Kato, Efficient Langevin simulation of coupled classical fields and fermions, Phys. Rev. B **88,** 235101 (2013).